Journal of The Electrochemical Society, **147** (10) 3801-3807 (2000)
S0013-4651(00)02-088-7 CCC: $7.00 © The Electrochemical Society, Inc.

Anion Transport in Prussian Blue Films in Acetonitrile and Propylene Carbonate Solutions

Hochun Lee,[a] Haesik Yang,[b,*] Youn Tae Kim,[b] and Juhyoun Kwak[a,*,z]

[a]*Department of Chemistry and School of Molecular Science, Korea Advanced Institute of Science and Technology, Taejon 305-701, Korea*
[b]*Electronics Telecommunication Research Institute, Microsystem Team, Taejon 305-600, Korea*

The mass transport behavior of Prussian blue (PB) films in acetonitrile (AN) and propylene carbonate (PC) solutions has been revealed using the cyclic electrochemical quartz crystal microbalance (EQCM) technique and the electrochemical/electrogravimetric impedance technique. It was found that cation transport is dominant during the redox reaction of PB films in AN solutions, whereas anion as well as cation takes part in ion transport in PC solutions. It was also found that anion transport is greater in a Li^+-containing solution than in a Na^+-containing solution. These results are discussed in terms of zeolitic structure of PB films and ionic mobility. Moreover, using the electromechanical impedance technique, it was shown that the morphological change during the redox reaction of PB films is not significant.

Manuscript submitted February 23, 2000; revised manuscript received June 27, 2000.

Prussian blue (PB) films have attracted much attention both in the fundamental and practical aspects because they serve as a good model system for studying the charge transport mechanism[1-3] and they can be applied to electrochromic devices,[4-6] rechargeable batteries,[7-9] ion selective sensors,[10,11] and electrocatalysts.[12-14] It is known that cation transport is dominant during the redox reaction of PB films and that the electroactivity and ion transport behavior of PB films are highly limited by their pore size because PB films have a rigid zeolitic structure; the electroactivity in aqueous solutions containing Na^+ or Li^+ is small while the electroactivity in solutions containing K^+, Rb^+, Cs^+, or NH_4^+ is large,[5,15,16] which results from larger hydration radius of Na^+ or Li^+ than the pore size of PB films.[5] Although there is still some controversy about the effect of anion on the redox reaction of PB films, some recent reports show that the role of the anion cannot be neglected completely for indium[17,18] and nickel[19] substituted analogues of PB films.

In contrast to the well-established knowledge in aqueous solutions, very little has been revealed on the charge-transport behavior in nonaqueous solutions. Crumbliss *et al.*[20] showed that the redox reactions of PB films in propylene carbonate (PC) solutions containing K^+, Na^+, and Li^+ are kinetically controlled by the diffusion of electrolytic cation. Leventis *et al.*[21] reported that PB films were stable upon electrochemical cycling in various nonaqueous solvents such as acetonitrile (AN), tetrahydrofuran, and dimethylformamide. Imanishi *et al.*[9] found that the water content in a PB film has a profound effect on the charge capacity when a PB film is used as a cathode of lithium batteries. It is noteworthy that PB films show electroactivities in aprotic solutions even containing Li^+ and Na^+, which is also very important in the view of their application to lithium batteries. However, there are few quantitative gravimetric studies on the mass-transport behavior of PB films in aprotic solutions.[22,23] Moreover, to our best knowledge, there has been no report for the presence of anion transport in aprotic solutions.

The electrochemical quartz crystal microbalance (EQCM) technique[24,25] has been widely employed to monitor the mass-transport behavior of thin-film-modified electrodes. In addition, the electrochemical/electrogravimetric impedance technique[26,27] has been found very useful in studying mass-transport behavior when more than two kinds of ionic species are involved in a redox reaction.[28-30]

In this study, the mass-transport behavior of PB films in anhydrous AN and PC solutions has been studied using the cyclic EQCM technique and the electrochemical/electrogravimetric impedance technique. It is known that PB is reduced to Everitt's salt (ES) or oxidized to Prussian white (PW). The reaction between PB and ES has been of major interest because both forms are very stable and the reaction is a reversible process.[15,33,34] Therefore, we confined our experiments on the reaction between PB and ES. First, the linear relation between the mass change of a PB film and the resonant frequency change of a quartz crystal is verified using the electromechanical impedance technique.[35-37] Second, mass-transport behaviors in Na^+- or Li^+-containing AN and PC solutions are investigated by using the cyclic EQCM technique. To reveal the effect of the anion or cation, we used three different salts of $NaClO_4$, $NaBPh_4$, and $LiClO_4$. Third, from the electrochemical/electrogravimetric impedance data, we examined the contribution of anion transport and obtained the relative diffusion coefficients of ions. Finally, the ion transport behavior was discussed in connection with the sizes of solvated ions, ionic conductivities, and zeolitic structure of PB films.

Experimental

Chemicals.—$FeCl_3$, $K_3[Fe(CN)_6]$, $NaClO_4$, $NaBPh_4$, $LiClO_4$, AN (anhydrous, 99.8%), and PC (anhydrous, 99.7%) were purchased from Aldrich and used as received. All the electrolytes were of reagent grade and dried at 80°C under vacuum before use.

Electrochemistry and film preparation.—The experimental apparatus, the electrochemical cell, and the electrodes used in this study were the same as those reported previously.[32,38] Ag/AgCl in 3 M NaCl was used as a reference electrode in aqueous solutions. Ag/Ag^+ in an AN or a PC solution was used as a reference electrode in AN or PC solutions whose potentials were +102 mV and −152 mV *vs.* SCE, respectively. PB films were electrodeposited from an aqueous solutions containing 0.1 M K_2SO_4, 5 mM $FeCl_3$, and 5 mM $K_3[Fe(CN)_6]$ by cycling potential between 0.6 to 0.35 V. For all films in this study, the cycling was continued until about 120 $\mu g\ cm^2$ was obtained. PB has been described in two compositions, the soluble form, $KFe^{III}[Fe^{II}(CN)_6]$, and the insoluble form, $Fe^{III}_4[Fe^{II}(CN)_6]_3 \cdot 6H_2O$. The as-grown films are assumed to be the insoluble form because the energy dispersive X-ray analysis (EDX) reveals no K^+. After polymerization, the cell and the film were washed with plenty of pure solvent and transferred into an Ar-filled glove box. The cyclic EQCM and the electrochemical/electrogravimetric impedance experiments were performed in the glove box, and the electromechanical impedance experiments were performed in atmosphere in a closed cell. All the electrolyte concentrations were fixed as 1 M. All data in the cyclic EQCM experiments were measured during the second cycle of two consecutive cycles after being held at the positive potential limit. Scan rate was 10 mV s^{-1} for all the cases. The electromechanical impedance data and the electrochemical/electrogravimetric impedance data were fitted using the

* Electrochemical Society Active Member.
z E-mail: jhkwak@kaist.ac.kr

S0013-4651(00)02-088-7 CCC: $7.00

complex nonlinear least-squares (CNLS) fitting program. The CNLS program used in this work is the LEVM program (Scribner, VA).

Results and Discussion

Relation between mass change and resonance frequency.—The linear relationship between the mass change of a film (ΔM) and the resonance frequency change of a quartz crystal (Δf_o) is valid only for an elastic film because Δf_o is influenced not only by ΔM but also the total resistance of a quartz crystal (R_t) that depends on the morphological changes (viscoelastic change and volume change) of a film.[35-37] In our previous report,[38] we showed that the linear relationship between ΔM and Δf_o can be proved by comparing Δf_o with the maximum-conductance frequency change (Δf_r) obtained from the electromechanical impedance. Figure 1 shows the result of the electromechanical impedance technique during the cyclic multipotential step experiments for a PB film in 1 M $NaClO_4$/AN. As shown in Fig. 1a, the Δf_o behavior is very similar to the Δf_r behavior. R_t shown in Fig. 1b varies within 15 Ω. It is very small compared to that for polypyrrole films reported in our previous studies,[38,39] which implies that the morphology change is not significant. It has been pointed out that the swelling/de-swelling of PB films during their redox reaction is not serious owing to their rigid structure.[18,40] Thus, for all the experiments in this study, ΔM can be obtained from Δf_o without consideration of the morphological changes of PB films.

Mass-transport behavior in acetonitrile solutions.—There are two methods for correlating the electric response and gravimetric response. The first one is to compare charge change (ΔQ) and mass change (ΔM), which has been usually used in many EQCM studies. In this method, the average apparent molar mass of charge compensating species per charge (W'_{avg}) is obtained by Eq. 1

$$W'_{avg} = F(\Delta M_t/\Delta Q_t) \quad [1]$$

where F is the Faraday constant, and ΔM_t and ΔQ_t are the total mass change and the total charge change, respectively, at the anodic or the cathodic scan. The second one is to compare current (I) and normalized mass change rate (G_n), which are time-derivatives of ΔQ and ΔM, respectively. G_n is obtained from the mass change rate ($G = dM/dt$) according to Eq. 2

$$G_n = -(zF/W')G \quad [2]$$

where z is the charge of an ion and W' is the apparent molar mass of charge-compensating species. If G_n is larger than I at any potential, it means that the real W' value is larger than the given W'. This method has been found very useful for monitoring potential-dependent mass transport as shown in our previous reports.[31,32,38,41] We employed both methods in the following discussion for the cyclic EQCM experiments.

Figure 2 shows cyclic voltammograms, ΔM, and G_n diagrams obtained from the cyclic EQCM experiments for PB films in AN solutions. In the cyclic voltammogram for a PB film in $NaClO_4$/AN (Fig. 2a), ΔM increases monotonically in the cathodic scan and decreases in the anodic scan. This implies that cation transport is dom-

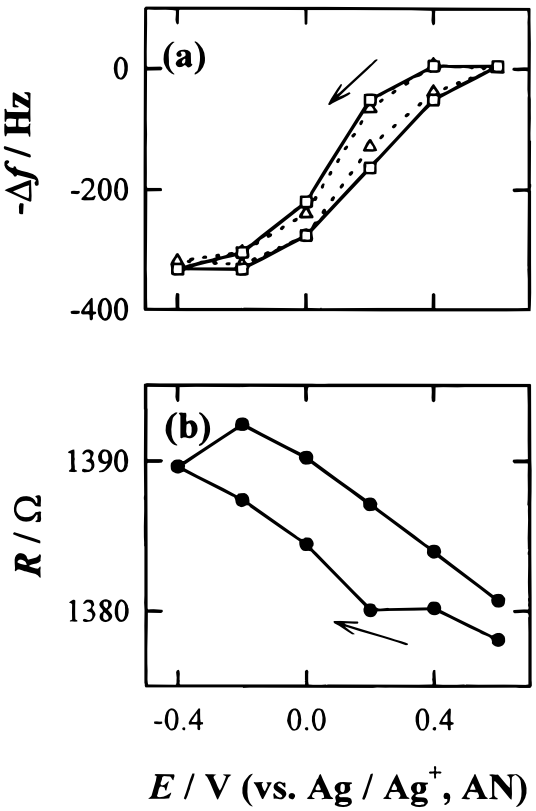

Figure 1. (a) f_r (—□—), f_o (···△···) changes and (b) R_t change for a PB film in 1 M $NaClO_4$/AN during the electromechanical impedance experiment.

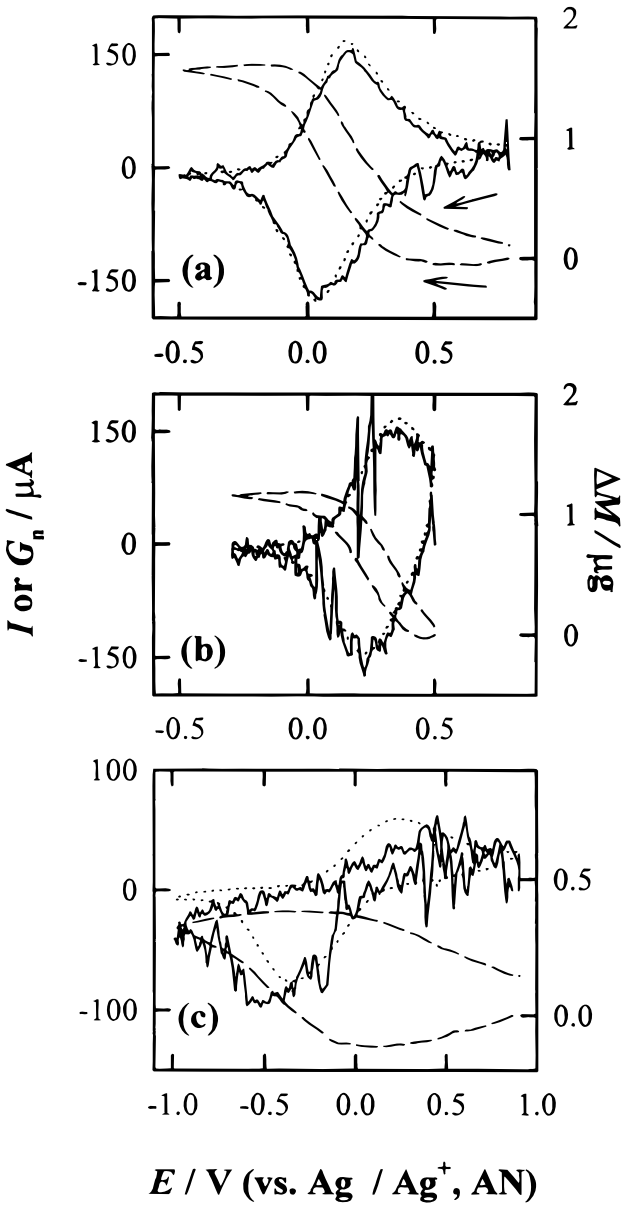

Figure 2. Cyclic voltammograms (I *vs.* E; ···), normalized mass change rate diagrams (G_n *vs.* E; —), and mass change diagrams (ΔM *vs.* E; - - -) for a PB film in (a) $NaClO_4$/AN, (b) $NaBPh_4$/AN, and (c) $LiClO_4$/AN.

S0013-4651(00)02-088-7 CCC: $7.00

inant. W'_{avg} at the cathodic scan in Fig. 2a is 23.1, which is very similar to the molar mass of Na^+ (W_{Na^+}). In all the following experiments, W'_{avg} at the anodic scan is similar to that at the cathodic scan within an experimental error. Therefore, only W'_{avg} at the cathodic scan was given in Table I. In the G_n diagram, when W_{Na^+} is regarded as W', G_n is very similar to I over the whole potential range. These indicate that the charge-compensating species is only Na^+ irrespective of the redox state of a PB film. To examine the effect of the anion, a cyclic EQCM experiment was performed for a PB film in $NaBPh_4$/AN (Fig. 2b). Because of an irreversible current rise that seems to be related to BPh_4^- decomposition, the positive potential limit of the cyclic voltammogram was reduced in comparison with Fig. 2a. Except that the redox potential is shifted by about +0.2 V, the cyclic voltammogram in Fig. 2b shows a similar shape to that in Fig. 2a. The mass-transport behavior in Fig. 2b is nearly the same as that in Fig. 2a. W'_{avg} is 23.2 and G_n is similar to I over the whole potential range when the molar mass of W_{Na^+} is regarded as W'. If there were anion or neutral salt transport, the mass transport behavior would vary with an electrolytic anion. From these results, it is obvious that there is only Na^+ transport, and the transport of anion or neutral species (solvent, salt) is negligible during the redox reaction of a PB film in Na^+-containing AN solutions. For a PB film in $LiClO_4$/AN (Fig. 2c), the cyclic voltammogram was obtained after several cycles because peak currents are decreased and peak separation becomes larger during the first few cycles. This might be due to the structural change by lithium insertion[9] or due to the formation of a passive layer on the film surface that hinders the ion transport across it. Leventis *et al*.[21] reported very symmetrical cyclic voltammograms for PB films in both $NaClO_4$/AN and $LiCF_3SO_3$/AN. We also observed that cyclic voltammograms became more symmetrical in AN solutions containing 1 vol % water. Therefore, the result of Leventis *et al*.[21] seems to result from the trace water in the electrolyte solutions. The ΔM diagram of Fig. 2c shows that cation transport prevails as in Fig. 2a and b. W'_{avg} at the cathodic scan in Fig. 2c is 7.9, which is slightly larger than the molar mass of Li^+ (W_{Li^+}). When the molar mass of W_{Li^+} is regarded as W', G_n is smaller than I in the beginning and then becomes much larger beyond the peak potential at the cathodic scan. Thus, it can be said that although the contribution of anion or neutral species cannot be thoroughly neglected, Li^+ transport is dominant during the redox reaction of a PB film in Li^+-containing AN solutions. In brief, based on the results of Fig. 2, it is evident that the mass transport behavior of PB films in AN solutions is mainly controlled by cation transport.

Mass-transport behavior in propylene carbonate solutions.— Figure 3 shows the cyclic EQCM results for PB films in PC solutions. A PB film in $NaClO_4$/PC (Fig. 3a) shows a stable and reversible cyclic voltammogram. ΔM increases monotonically in the cathodic scan and decreases in the anodic scan, which is similar to that observed for a PB film in $NaClO_4$/AN (Fig. 2a). However, W'_{avg} is 17.9, which is smaller than W_{Na^+}. In addition, G_n is much smaller than I around the peak potentials when W_{Na^+} is regarded as W'. This implies that other species move in the opposite direction to Na^+ transport. Those species can be anion, solvent, or neutral salt. To show this more clearly, a PB film in $NaBPh_4$/PC (Fig. 3b) was investigated. The cyclic voltammogram in Fig. 3b is stable but shows very large peak separation as compared with that in Fig. 3a. W'_{avg} in Fig. 3b is 10.5, which is smaller than W'_{avg} in Fig. 3a. In addition, G_n is much smaller than I in most of the potential range, when W_{Na^+} is regarded as W'. The fact that W'_{avg} changes with the kind of anion proves the presence of anion or neutral salt transport. In the present state, however, it is impossible to reveal which one of the two is really present. The cyclic voltammogram for a PB film in $LiClO_4$/PC (Fig. 3c) is very stable and reversible. It is in contrast with a PB film in $LiClO_4$/AN (Fig. 2c), in which the cyclic voltammogram is unstable with large peak separation. The ΔM diagram of Fig. 3c shows clearly that both cation and anion transports occur. ΔM decreases in the beginning and then increases around the peak potential at the cathodic scan. This indicates that the anion moves out of the film, and then the cation moves into the film. In Fig. 3c, W'_{avg}

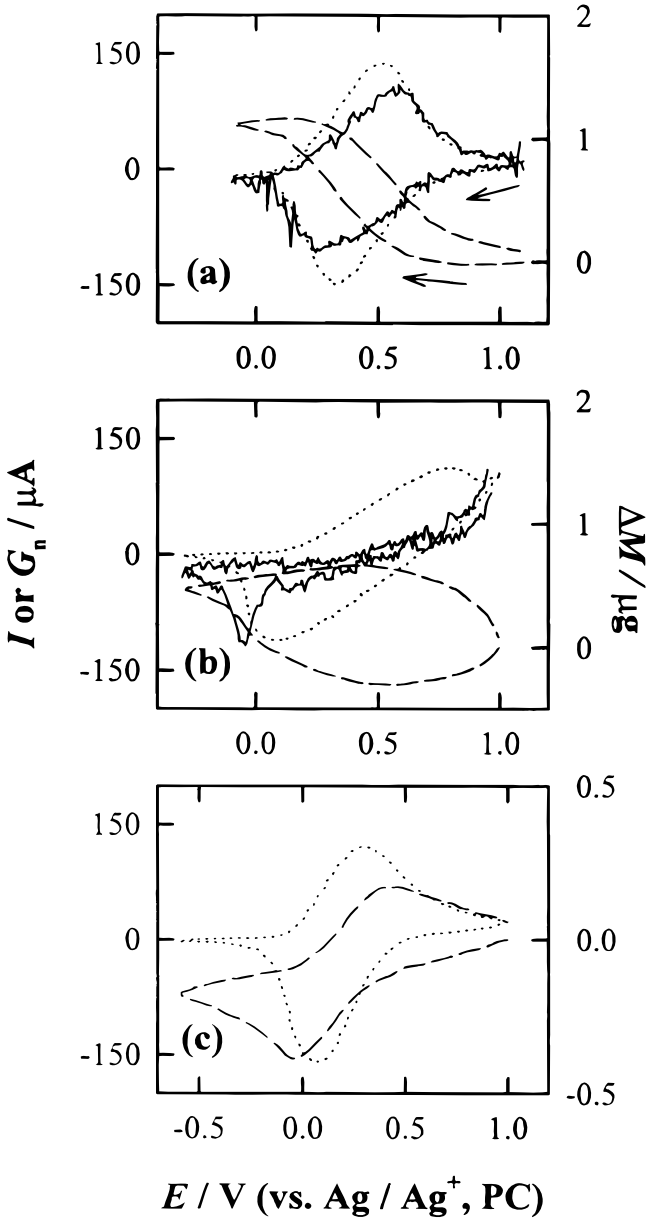

Figure 3. (a) Cyclic voltammograms (I *vs.* E; ⋯),normalized mass change rate diagrams (G_n *vs.* E; —), and mass change diagrams (ΔM *vs.* E; - - -) for a PB film in (a) $NaClO_4$/PC, (b) $NaBPh_4$/PC, and (c) $LiClO_4$/PC.

cannot be calculated because the relation of ΔQ and ΔM is not linear at both cathodic and anodic scans. Instead, W' values are obtained by adjusting G_n to I at 0.3 and 0.25 V, and regarded as W'_+ and W'_-, respectively. As shown in Table I, W'_+ is 23.7 that is much larger than W_{Li^+}, which means that Li^+ transport is accompanied by some solvent (PC) transport. W'_- is 5.8 that is much smaller than $W_{ClO_4^-}$. Although an exact explanation is impossible, this might be due to cation and solvent transport occurring even in the range where anion transport prevails. In contrast with our results, Aoki *et al*.[22,23] reported that Na^+ or Li^+ transport occurs dominantly over ClO_4^- transport for PB films in PC solutions containing 1.5 wt % water. We also observed that cation transport becomes more dominant in PC solutions containing a small amount of water. Thus, the different ion transport behaviors can be ascribed to the water content in solutions. Conclusively speaking, the mass-transport behavior of PB films in PC solutions is influenced by not only cation transport but also anion transport.

Electrochemical/electrogravimetric impedance technique.—Figure 4a shows the equivalent circuit for an electrode/polymer film/

S0013-4651(00)02-088-7 CCC: $7.00

Table I. W'_{avg} values obtained from cyclic EQCM experiments.

Electrolyte	W_+ [a]	W_- [b]	W'_{avg} [c]	W'_+ [d]	W'_- [e]
$NaClO_4$/AN	23	99.5	23.1		
$NaBPh_4$/AN	23	319	23.2		
$LiClO_4$/AN	6.9	99.5	7.9		
$NaClO_4$/PC	23	99.5	17.9		
$NaBPh_4$/PC	23	319	10.5		
$LiClO_4$/PC	6.9	99.5		23.7	5.8

[a] Molar mass of a cation (g mol^{-1}).
[b] Molar mass of an anion (g mol^{-1}).
[c] $W'_{avg} = F(\Delta M/\Delta Q)$ during the cathodic scan (g mol^{-1}).
[d] $W'_+ = F(G/I)$ at -0.3 V *vs*. Ag/Ag^+ (PC).
[e] $W'_- = F(G/I)$ at 0.25 V *vs*. Ag/Ag^+ (PC).

electrolyte solution system, where R_s is the solution resistance, C_d is the double-layer capacitance in the electrode/polymer or the polymer/solution interface, R_{ct} is the charge-transfer resistance, and Z' is an impedance related to the charge transport in a film. When the time scale of the ion diffusion process differs from that of the charge-transfer phenomena, the circuit of Fig. 4a shows the same electrical response as that of Fig. 4b.[42] The latter circuit has the advantage of an easier computational management.[42] If only one kind of ion transport takes part in ion transport, which is much slower than electron transport, Z' is simplified to Z_D (Fig. 4c) of which the mathematical form is given by

$$Z_D = R_D \frac{\coth\sqrt{j\omega R_D C_D}}{\sqrt{j\omega R_D C_D}} \quad [3]$$

where R_D is the ionic resistance, C_D is the redox capacitance in a film, j is $\sqrt{-1}$, and ω is an angular frequency.[43-45] As shown in Fig. 5a and b, the electrogravimetric capacitance ($\Delta M/\Delta E$) plot for Z_D appears in the third or the first quadrant when ion transport is cation-specific or anion-specific, respectively. If dual ion transport takes place, Z' is given as the parallel combination of Z_{D+} and Z_{D-} (Fig. 4d), where Z_{D+} represents Z_D for cation transport and Z_{D-} represents Z_D for anion transport. ($\Delta M/\Delta E$) plots for the parallel combination of Z_{D+} and Z_{D-} is shown from Fig. 5c to f in terms of C_D and R_DC_D values.[31]

To obtain the faradaic electrochemical capacitance ($\Delta Q^f/\Delta E^f$) and the faradaic electrogravimetric capacitance ($\Delta M^f/\Delta E^f$), the effect of R_s, R_{ct}, and C_d on the capacitance data must be corrected. As shown in Fig. 4b, the ratio of the faradaic potential (ΔE^f) to the applied potential (ΔE) is equal to Z'/Z, where Z is ($\Delta E/\Delta I$). Z'/Z is determined by obtaining the values of R_s, R_{ct}, and C_d from the fitting of Z to the adequate equivalent circuit such as Fig. 4b. Because, in the circuit of Fig. 4b, the charge change due to faradaic process (ΔQ^f) is equal to ΔQ and the mass change due to faradaic process (ΔM^f) is equal to ΔM, ($\Delta Q^f/\Delta E^f$) and ($\Delta M^f/\Delta E^f$) are represented as follows

$$\left(\frac{\Delta Q^f}{\Delta E^f}\right) = \left(\frac{\Delta Q}{\Delta E}\right)\left(\frac{\Delta E}{\Delta E^f}\right) = \left(\frac{\Delta Q}{\Delta E}\right)\left(\frac{Z'}{Z}\right) \quad [4]$$

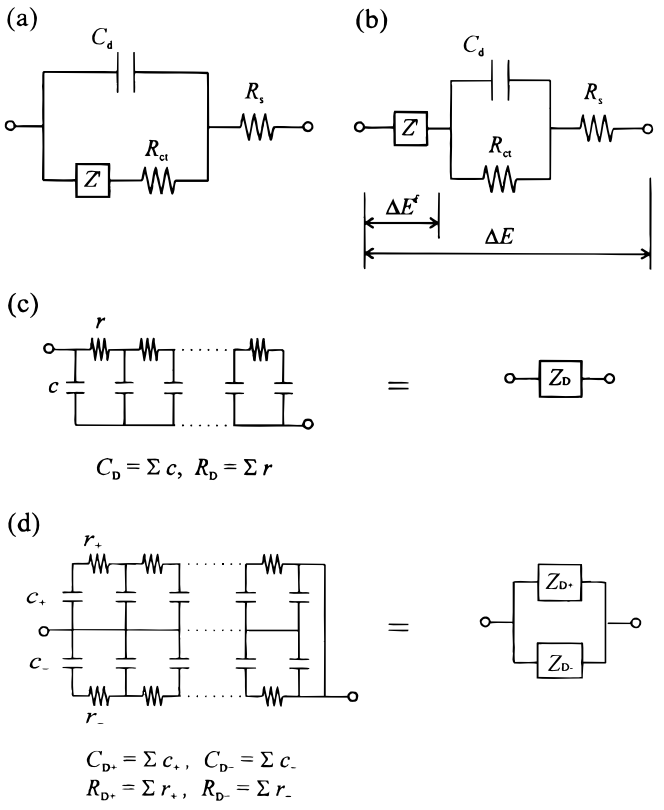

Figure 4. (a) Equivalent circuit for an electrode/polymer film/electrolyte solution system: R_s, solution resistance; R_{ct}, charge-transfer resistance; C_d, double-layer capacitance; Z', the charge-transport impedance in a polymer film. (b) Z' in the case in which one kind of ion transport occurs, and (c) Z' in the case in which both cation and anion transport occurs. Z_{D+} represents Z_D for cation transport and Z_{D-} represents Z_D for anion transport.

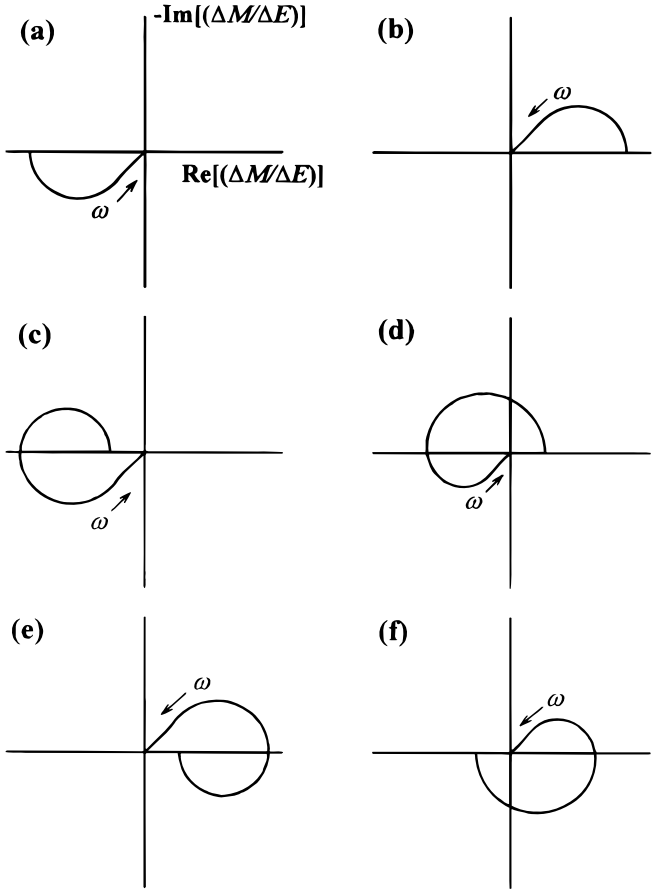

Figure 5. Electrogravimetric capacitance ($\Delta M/\Delta E$) plots for Z_D in the case in which ion transport is (a) $C_{D+} \neq 0$, $C_{D-} = 0$ (cation-specific), (b) $C_{D+} = 0$, $C_{D-} \neq 0$ (anion-specific), (c) $R_{D+}C_{D+} < R_{D-}C_{D-}$ and $-(W'/z_+F)C_{D+} > -(W'/z_-F)C_{D-}$, (d) $R_{D+}C_{D+} < R_{D-}C_{D-}$ and $-(W'/z_+F)C_{D+} < -(W'/z_-F)C_{D-}$, (e) $R_{D+}C_{D+} > R_{D-}C_{D-}$ and $-(W'/z_+F)C_{D+} < -(W'/z_-F)C_{D-}$, and (f) $R_{D+}C_{D+} > R_{D-}C_{D-}$ and $-(W'/z_+F)C_{D+} > -(W'/z_-F)C_{D-}$.

S0013-4651(00)02-088-7 CCC: $7.00

$$\left(\frac{\Delta M^{\mathrm{f}}}{\Delta E^{\mathrm{f}}}\right)=\left(\frac{\Delta M}{\Delta E}\right)\left(\frac{\Delta E}{\Delta E^{\mathrm{f}}}\right)=\left(\frac{\Delta M}{\Delta E}\right)\left(\frac{Z'}{Z}\right) \quad [5]$$

When both cation transport and anion transport are present, $(\Delta Q_{+}^{\mathrm{f}}/\Delta E^{\mathrm{f}})$ and $(\Delta Q_{-}^{\mathrm{f}}/\Delta E^{\mathrm{f}})$ can be obtained by solving the following two equations

$$\left(\frac{\Delta Q^{\mathrm{f}}}{\Delta E^{\mathrm{f}}}\right)=\left(\frac{\Delta Q_{+}^{\mathrm{f}}}{\Delta E^{\mathrm{f}}}\right)+\left(\frac{\Delta Q_{-}^{\mathrm{f}}}{\Delta E^{\mathrm{f}}}\right) \quad [6]$$

$$\left(\frac{\Delta M^{\mathrm{f}}}{\Delta E^{\mathrm{f}}}\right)=\left(\frac{\Delta M_{+}^{\mathrm{f}}}{\Delta E^{\mathrm{f}}}\right)+\left(\frac{\Delta M_{-}^{\mathrm{f}}}{\Delta E^{\mathrm{f}}}\right)=-\frac{W_{+}'}{z_{+}F}\left(\frac{\Delta Q_{+}^{\mathrm{f}}}{\Delta E^{\mathrm{f}}}\right)-\frac{W_{-}'}{z_{-}F}\left(\frac{\Delta Q_{-}^{\mathrm{f}}}{\Delta E^{\mathrm{f}}}\right) \quad [7]$$

However, when only one kind of ion transport is present, $(\Delta Q/\Delta E)$ and $(\Delta M/\Delta E)$ can be compared without considering the effect of R_{s}, R_{ct}, and C_{d} as follows

$$\left(\frac{\Delta M}{\Delta E}\right)=\left(\frac{\Delta E^{\mathrm{f}}}{\Delta E}\right)\left(\frac{\Delta M^{\mathrm{f}}}{\Delta E^{\mathrm{f}}}\right)=-\frac{W'}{zF}\left(\frac{\Delta E^{\mathrm{f}}}{\Delta E}\right)\left(\frac{\Delta Q^{\mathrm{f}}}{\Delta E^{\mathrm{f}}}\right)=-\frac{W'}{zF}\left(\frac{\Delta Q}{\Delta E}\right) \quad [8]$$

Figure 6 shows $(\Delta Q/\Delta E)_{\mathrm{n}}$ plots and simultaneously obtained $(\Delta M/\Delta E)$ plots for PB films in AN solutions. In Fig. 6a, $(\Delta M/\Delta E)$ plot appears only in the third quadrant, which indicates that ion transport may be cation specific. When W' is regarded as W_{Na^+}, the $(\Delta Q/\Delta E)_{\mathrm{n}}$ [$= -(W'/zF)(\Delta Q/\Delta E)$] plot shows good agreement with the $(\Delta M/\Delta E)$ plot. A PB film in $NaBPh_4$/AN (Fig. 6b) also shows good agreement between $(\Delta Q/\Delta E)_{\mathrm{n}}$ and $(\Delta M/\Delta E)$ plots, when W' is regarded as W_{Na^+}. In addition, it is noteworthy that the plots of Fig. 6b are very similar to those of Fig. 6a. If the charge compensating species were different, the plots would be quite different from each other in their semicirclar size because of different molar masses of charge-compensating species. These mean that there is only Na^+ transport, which confirms the result obtained in the cyclic EQCM experiments.

Figure 7 shows the electrochemical/electrogravimetric impedance data for PB films in $NaClO_4$/PC. In Fig. 7b, the $(\Delta M/\Delta E)$ plot appears through the first, the fourth, and the third quadrant as the measuring frequency decreases. This implies that anion transport is considerable in the higher frequency region, whereas cation transport is considerable in the lower frequency region. Figure 7c and d show $(\Delta Q^{\mathrm{f}}/\Delta E^{\mathrm{f}})$ and $(\Delta W^{\mathrm{f}}/\Delta E^{\mathrm{f}})$ plots, respectively. In this case, the exact value of (W'/z) values are not known. However, if the results in AN solutions are considered, (W_{+}'/z) value seems not to be very different from $(W_{\mathrm{Na}^+}/+1)$. Moreover, (W_{-}'/z) value will not be significantly different from $(W_{\mathrm{ClO_4^-}}/-1)$ owing to the poor solvation of the anion in aprotic solvent such as PC. As shown in Fig. 7c and d, although $(\Delta Q_{-}^{\mathrm{f}}/\Delta E^{\mathrm{f}})$ and $(\Delta M_{-}^{\mathrm{f}}/\Delta E^{\mathrm{f}})$ plots are a little noisy, it is evident that anion transport is present for a PB film in $NaClO_4$/PC. The noise of data is partly related to small Z'/Z ratio due to relatively large R_{s} and R_{ct}. The smaller Z'/Z ratio is, the smaller ΔE^{f} and ΔM^{f} are. Figure 8a and b show $(\Delta Q^{\mathrm{f}}/\Delta E^{\mathrm{f}})$ and $(\Delta M^{\mathrm{f}}/\Delta E^{\mathrm{f}})$ plots for a PB film in $NaBPh_4$/PC, and Fig. 8c and d show the plots for a PB film in $LiClO_4$/PC. In these cases, $(W_{\mathrm{Na}^+}/+1)$ and $(W_{\mathrm{BPh_4^-}}/-1)$ [or

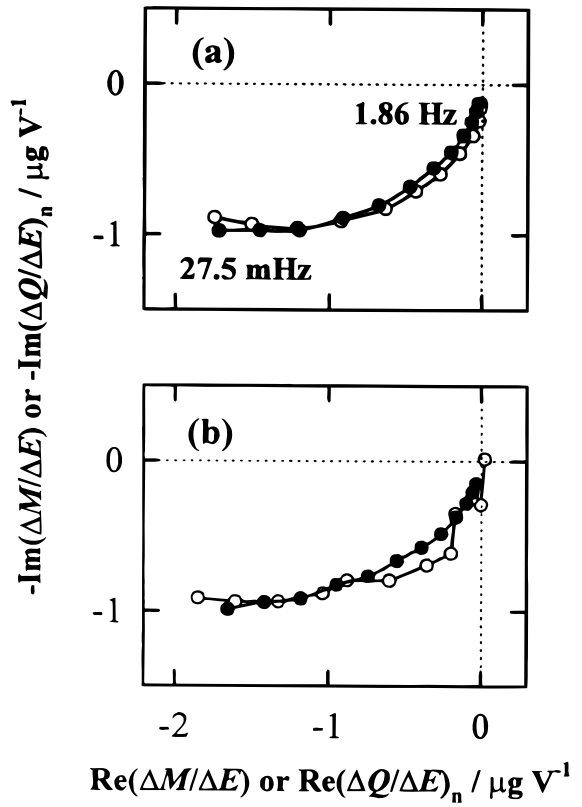

Figure 6. Electrogravimetric capacitance ($\Delta M/\Delta E$; ○) plots and normalized electrochemical capacitance [$\Delta Q/\Delta E)_{\mathrm{n}} = -(W'zF)(\Delta Q/\Delta E)$; ●] plots for a PB film in (a) $NaClO_4$/AN at $E = 0.1$ V, and (b) $NaBPh_4$/AN at $E = 0.3$ V.

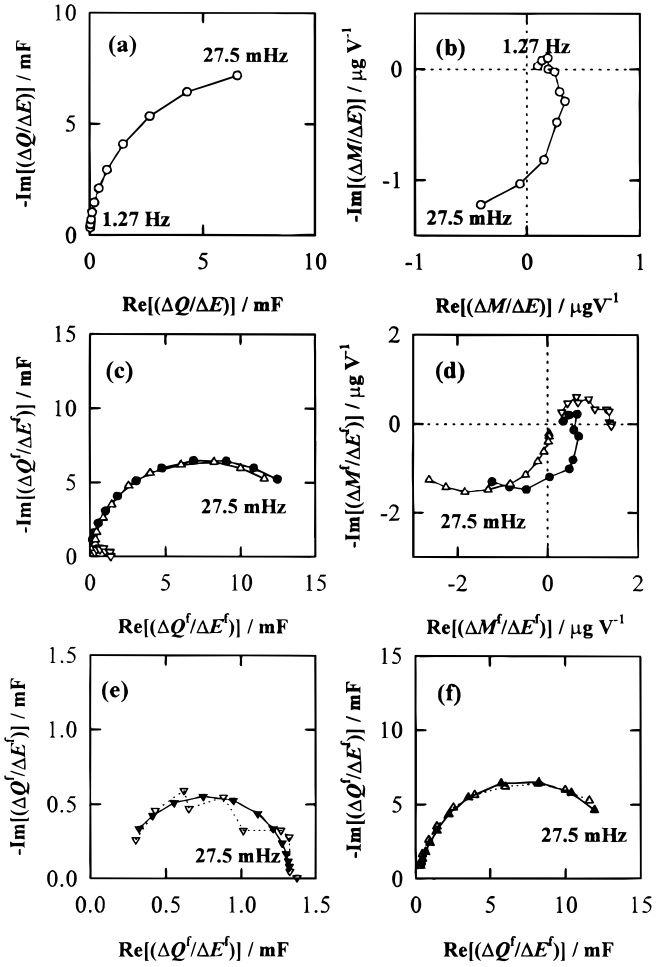

Figure 7. (a) Electrochemical capacitance ($\Delta Q/\Delta E$) plot, (b) electrogravimetric ($\Delta M/\Delta E$) plot, (c, e, f) faradaic electrochemical capacitance ($\Delta Q^{\mathrm{f}}/\Delta E^{\mathrm{f}}$) plots, and (d) faradaic electrogravimetric capacitance ($\Delta M^{\mathrm{f}}/\Delta E^{\mathrm{f}}$) plots at $E = 0.45$ V for a PB film in $NaClO_4$/PC ($W_{+}' = W_{\mathrm{Na}^+}$ and $W_{-}' = W_{\mathrm{ClO_4^-}}$); ($\Delta Q/\Delta E$) and ($\Delta M/\Delta E$) (○), ($\Delta Q^{\mathrm{f}}/\Delta E^{\mathrm{f}}$) and ($\Delta M^{\mathrm{f}}/\Delta E^{\mathrm{f}}$) (●), ($\Delta Q_{+}^{\mathrm{f}}/\Delta E^{\mathrm{f}}$) and ($\Delta M_{+}^{\mathrm{f}}/\Delta E^{\mathrm{f}}$) (△), ($\Delta Q_{-}^{\mathrm{f}}/\Delta E^{\mathrm{f}}$) and ($\Delta M_{-}^{\mathrm{f}}/\Delta E^{\mathrm{f}}$) (▽), simulated ($\Delta Q_{+}^{\mathrm{f}}/\Delta E^{\mathrm{f}}$) (▲), and simulated ($\Delta Q_{-}^{\mathrm{f}}/\Delta E^{\mathrm{f}}$) (▼).

S0013-4651(00)02-088-7 CCC: $7.00

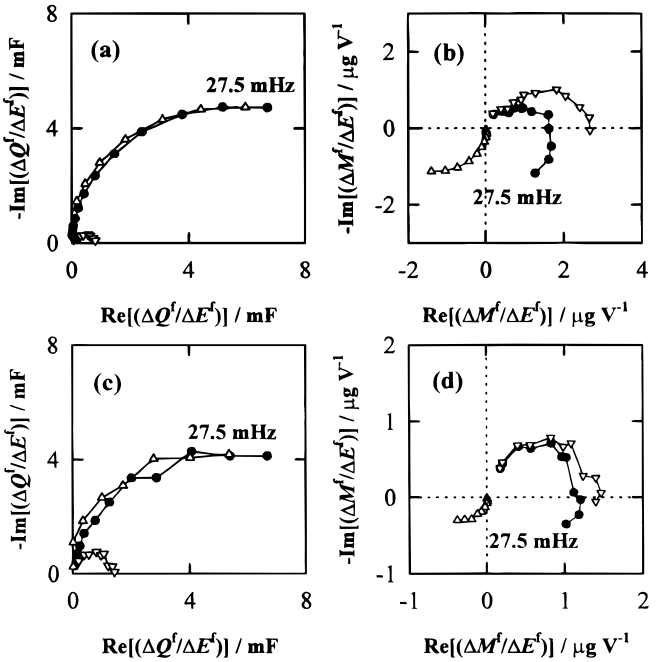

Figure 8. (a, c) Faradaic electrochemical capacitance ($\Delta Q^f/\Delta E^f$) plots and (b, d) faradaic electrogravimetric capacitance ($\Delta M^f/\Delta E^f$) plots for PB films in (a, b) $NaBPh_4$ at E = 0.45 V ($W'_+ = W_{Na^+}$ and $W'_- = W_{BPh_4^-}$) and (c, d) $LiClO_4$ at E = 0.15 V ($W'_+ = W_{Li^+}$ and $W'_- = W_{ClO_4^-}$); ($\Delta Q^f/\Delta E^f$) and ($\Delta M^f/\Delta E^f$) (●), ($\Delta Q^f_+/\Delta E^f$) and ($\Delta M^f_+/\Delta E^f$) (△), and ($\Delta Q^f_-/\Delta E^f$) and ($\Delta M^f_-/\Delta E^f$) (▽).

($W_{Li^+}/+1$) and ($W_{ClO_4^-}/-1$)] are regarded as (W'_+/z) and (W'_-/z), respectively. It is clear that anion transport is considerable in both cases, too. These results clearly prove that anion transport is responsible for the smaller W'_{avg} values obtained in the cyclic EQCM experiments in PC solutions.

The equivalent circuit of Fig. 4c is used to fit ($\Delta Q^f_+/\Delta E^f$) and ($\Delta Q^f_-/\Delta E^f$) plots, and the values of fitted parameters (C_D and R_DC_D) are given in Table II. For both cation and anion, R_DC_D values for a PB film in $NaBPh_4$/PC are larger than that in $NaClO_4$/PC. This means a slower diffusion process of ions in the former case, which explains why peak separation in the cyclic voltammogram in $NaBPh_4$/PC (Fig. 3b) is larger than that in $NaClO_4$/PC (Fig. 3a). $R_{D+}C_{D+}$ value in $LiClO_4$/PC is similar to that in $NaBPh_4$/PC whereas $R_{D-}C_{D-}$ value is smaller than that in $NaBPh_4$/PC. In the cyclic voltammogram in $LiClO_4$/PC (Fig. 3c), the peak separation is much smaller than that in Fig. 3b. Therefore, the smaller peak separation in Fig. 3c seems to be due to the larger diffusion coefficient of an anion.

In Table II, the C_D ratio of anion to cation (C_{D-}/C_{D+}) and the R_DC_D ratio of cation to anion ($R_{D+}C_{D+}/R_{D-}C_{D-}$) are given. It is noteworthy that both (C_{D-}/C_{D+}) and ($R_{D+}C_{D+}/R_{D-}C_{D-}$) are increasing in the following order

$$NaBPh_4/PC \fallingdotseq NaClO_4/PC < LiClO_4/PC \quad [9]$$

Among the three cases, a PB film in $LiClO_4$/PC shows the largest ($R_{D+}C_{D+}/R_{D-}C_{D-}$), which seems to be due to the slow diffusion process of Li^+. It is known that the ionic conductivity of Li^+ is smaller than that of Na^+ owing to large solvation sphere in PC solutions.[20,46]

Relation between ion transport and PB structure.—From the results in the previous sections, the redox reaction between PB and ES can be written as below

$$1/4[Fe_4^{III}[Fe^{II}(CN)_6]_3\,(MA)_x\cdot 6H_2O] + e^- + (1-x)M^+ \leftrightarrow 1/4[MFe_4^{II}[Fe^{II}(CN)_6]_3\cdot 6H_2O] + xA^- \quad [10]$$

where M^+ is Na^+ or Li^+, A^- is ClO_4^- or BPh_4^-, and x is the anionic contribution to the total ion transport. The x value is nearly zero in AN solutions, whereas it varies with the kinds of electrolyte in PC solutions. At this time, it is difficult to offer a clear reason for the absence/presence of anion transport in AN/PC solutions. One possibility is the difference in structures of PB films in AN and PC solutions. As mentioned, PB has zeolitic pores through which ion transport takes place during the redox reactions. The pore radius has been known to be *ca*. 1.6 Å.[5] However, it has been reported that the pore size is influenced by water molecules present within the films.[9,47] Thus, it seems to be possible that pore size in PC solutions is different from that in AN solutions because of the different solvation characteristics of AN and PC. Ionic radii of anions are larger than those of cations (Li^+: 0.6 Å, Na^+: 0.95 Å, ClO_4^-: 2.4 Å, and BPh_4^-: 4.2 Å)[46,48] Although the radii of solvation sphere of cations are comparable to those of bare anions, (Li^+: 2.97 Å in AN and 3.37 Å in PC, and Na^+: 3.08 Å in AN and 3.10 Å in PC),[48] it is well known that there is the partial removal of the solvation sphere when cations move into the PB films.[20,47] Therefore, it can be assumed that the pore size of PB films in PC solutions is large enough to accommodate both cation and anion transports whereas only a small cation takes part in the ion transport for PB films in AN solutions. An alternative explanation would take into account the ionic mobilities. It is known that the limiting molar conductivity ratio of anion to cation is always larger in PC solutions than in AN solutions.[46,48] This implies that the relative mobility of anion to cation is larger in PC solutions than in AN solutions. Moreover, the difference may be enhanced within the films because the physical/chemical environment within the films will be very different from that in solutions. Actually, as shown in Table II, the $R_{D+}C_{D+}$ values are three or seven times larger than $R_{D-}C_{D-}$ values. This means that the diffusion processes of anions are faster by three or seven times than those of cations, which cannot be understood when their molar conductivities in solutions are considered. It is known that the limiting molar conductivity of ClO_4^- is only two times larger than that of Na^+ or Li^+ and that of BPh_4^- is similar to that of Na^+ or Li^+ in PC solutions.[47,48] Thus, it is quite probable that abnormally fast anion transport plays a greater role in ion transport for PB films in PC solutions.

Conclusions

The redox reaction of PB films has been studied in Na^+- and Li^+-containing AN and PC solutions. Morphology change is not significant during the redox reaction of PB films and the linear relation between mass and frequency in a gravimetric measurement can

Table II. Values of the parameters obtained by fitting the electrochemical capacitance data.

Solution	E[a] (V)	Cation		Anion		$\frac{C_{D-}}{C_{D+}}$	$\frac{R_{D+}C_{D+}}{R_{D-}C_{D-}}$
		C_D (mF)	R_DC_D (s)	C_D (mF)	R_DC_D (s)		
$NaClO_4$/PC	0.45	13	3.4	1.3	1.1	0.09	3.1
$NaBPh_4$/PC	0.45	9.7	6.9	0.8	2.3	0.08	3.0
$LiClO_4$/PC	0.15	8.5	7.5	1.5	1.0	0.18	7.5

[a] *vs*. Ag/Ag^+ (PC).

S0013-4651(00)02-088-7 CCC: $7.00

be used without consideration of the morphological changes of PB films. Cation transport prevails for PB films in AN solutions. On the other hand, not only cation transport but also anion transport takes place in PC solutions. In addition, the contribution of anion transport is more significant in Li^+-containing solution than that in Na^+-containing solution, which seems to be due to the larger radius of solvated Li^+ than that of Na^+. The presence of anion transport in PC solutions is suggested to result from the different solvation characteristics or the ionic mobility for PB films in AN and PC solutions.

Acknowledgments

We are grateful to Micros and the Korea Advanced Institute of Science and Technology for financial support of this research.

Korea Advanced Institute of Science and Technology assisted in meeting the publication costs of this article.

References

1. B. J. Feldman and R. W. Murray, *Inorg. Chem*., **26**, 1702 (1987).
2. S. B. Moon, A. Xidis, and V. D. Neff, *J. Phys. Chem*., **97**, 1634 (1993).
3. D. C. Arnett, P. Vöhringger, and N. F. Scherer, *J. Am. Chem. Soc*., **117**, 12262 (1995).
4. K. Itaya, K. Shibayama, H. Akahoshi, and S. Toshima, *J. Appl. Phys*., **53**, 804 (1982).
5. K. Itaya, I. Uchida, and V. D. Neff, *Acc. Chem. Res*., **19**, 162 (1986).
6. N. Leventis and Y. C. Chung, *Chem. Mater*., **4**, 1415 (1992).
7. V. D. Neff, *J. Electrochem. Soc*., **132**, 1382 (1985).
8. K. Honda and H. Hayashi, *J. Electrochem. Soc*., **134**, 1330 (1987).
9. N. Imanishi, T. Morikawa, J. Kondo, Y. Takeda, O. Yamamoto, N. Kinugasa, and T. Yamagishi, *J. Power Sources*, **79**, 215 (1999).
10. M. Hartmann, E. W. Grabner, and P. Bergveld, *Sens. Actuators B*, **4**, 333 (1991).
11. M. R. Deakin and H. Byrd, *Anal. Chem*., **61**, 290 (1989).
12. K. Itaya, N. Shoki, and I. Uchida, *J. Am. Chem. Soc*., **106**, 3423 (1984).
13. K. Ogura and I. Yoshida, *Electrochim. Acta*, **32**, 1191 (1987).
14. A. A. Karyakin, O. V. Gitelmacher, and E. E. Karyakina, *Anal. Chem*., **67**, 2419 (1995).
15. K. Itaya, T. Ataka, and S. Toshima, *J. Am. Chem. Soc*., **104**, 4767 (1982).
16. C. A. Lundren and R. W. Murray, *Inorg. Chem*., **26**, 1702 (1987).
17. M. A. Malik, G. Horanyi, P. J. Kulesza, G. Inzelt, V. Kertesz, R. Schmidt, and E. Czirok, *J. Electroanal. Chem*., **452**, 57 (1998).
18. E. Csahók, E. Vieil, and G. Inzelt, *J. Electroanal. Chem*., **457**, 251 (1998).
19. J. Bacskai, K. Martinusz, E. Czirók, G. Inzelt, P. J. Kulesza, and M. A. Malik, *J. Electroanal. Chem*., **385**, 241 (1995).
20. A. L. Crumbliss, P. S. Lugg, and N. Morosoff, *Inorg. Chem*., **23**, 4701 (1984).
21. N. Leventis and Y. C. Chung, *J. Electrochem. Soc*., **138**, L21 (1991).
22. K. Aoki, T. Miyamoto, and Y. Ohsawa, *Bull. Chem. Soc. Jpn*., **62**, 1658 (1989).
23. Y. Ohsawa and K. Aoki, *Sens. Actuators B*, **13-14**, 556 (1993).
24. D. A. Buttry and M. D. Ward, *Chem. Rev*., **92**, 1355 (1992).
25. D. A. Buttry, in *Electroanalytical Chemistry*, Vol. 17, A. J. Bard, Editor, p. 1, Marcel Dekker, Inc., New York (1991).
26. S. Bourkane, C. Gabrielli, and M. Keddam, *Electrochim. Acta*, **34**, 1081 (1989).
27. C. Gabrielli and B. Tribollet, *J. Electrochem. Soc*., **141**, 1147 (1994).
28. S. Cordoba-Torresi, C. Gabrielli, M. Keddam, H. Takenouti, and R. Torresi, *J. Elecroanal. Chem*., **290**, 269 (1990).
29. C. Gabrieeli, M. Keddam, H. Perrot, and R. Torresi, *J. Electroanal. Chem*., **378**, 85 (1994).
30. O. Bohnke, B. Vuillemin, C. Gabrielli, M. Keddam, and H. Perrot, *Electrochim. Acta*, **40**, 2765 (1995).
31. H. Yang and J. Kwak, *J. Phys. Chem. B*., **102**, 1982 (1998).
32. H. Yang, H. Lee, Y. Kim, and J. Kwak, *J. Electrochem. Soc*., To be published.
33. D. E. Stilwell, K. H. Park, and M. H. Miles, *J. Appl. Elecrochem*., **22**, 325 (1992).
34. A. R. J. Navarro, R. Tamarit, and F. Vincente, *J. Elecroanal. Chem*., **360**, 55 (1993).
35. S. J. Martin, V. E. Granstaff, and G. C. Frye, *Anal. Chem*., **63**, 2272 (1991).
36. M. Yang and M. Thompson, *Anal. Chem*., **65**, 1158 (1993).
37. M. A. M. Noël and P. A. Topart, *Anal. Chem*., **66**, 484 (1994).
38. H. Yang and J. Kwak, *J. Phys. Chem. B*., **101**, 774 (1997).
39. H. Lee, H. Yang, and J. Kwak, *J. Electroanal. Chem*., **468**, 104 (1999).
40. V. Plichon and S. Besbes, *J. Electroanal. Chem*., **284**, 141 (1990).
41. H. Yang and J. Kwak, *J. Phys. Chem. B*., **101**, 4656 (1997).
42. P. Ferloni, M. Mastragostino, and L. Meneghello, *Electrochim. Acta*, **41**, 27 (1996).
43. G. L. Duffit and P. G. Pickup, *J. Chem. Soc., Faraday Trans*., **88**, 1417 (1992).
44. I. Rubinstein, E. Sabatati, and J. Rishpon, *J. Electrochem. Soc*., **134**, 3078 (1987).
45. W. J. Albery, C. M. Elliot, and A. R. Mount, *J. Electroanal. Chem*., **288**, 15 (1990).
46. J. Burgess, *Metal Ions in Solution*, p. 101, Halstead Press, New York (1978).
47. P. J. Kulesza, M. A. Malik, M. Berettoni, M. Giorgrtti, S. Zamponi, R. Schmidt, and R. Marassi, *J. Phys. Chem. B*, **102**, 1870 (1998).
48. M. Ue, *J. Electrochem. Soc*., **141**, 3336 (1994).